

A numerical analysis of the equivalent skeleton void ratio for silty sand

Bei-Bing Dai^{*1,2}, Jun Yang³, Xiao-Qiang Gu² and Wei Zhang⁴

¹School of Civil Engineering, Sun Yat-sen University, Guangzhou, 510275, China

²Department of Geotechnical Engineering & Key Laboratory of Geotechnical and Underground Engineering of the Ministry of Education, Tongji University, Shanghai, 200092 China

³Department of Civil Engineering, The University of Hong Kong, Hong Kong, China

⁴College of Water Conservancy and Civil Engineering, South China Agricultural University, Guangzhou, 510642, China

(Received October 2, 2018, Revised November 23, 2018, Accepted December 2, 2018)

Abstract. Recent research on the behavior of silty sand tends to advocate the use of equivalent skeleton void ratio to characterize the density state of this type of soil. This paper presents an investigation to explore the physical meaning of the equivalent skeleton void ratio by means of DEM simulations for assemblies of coarse and fine particles under biaxial shear. The simulations reveal that the distribution pattern of fine particles in the soil skeleton plays a crucial role in the overall macroscopic response: The contractive response observed at the macro scale is mainly caused by the movement of fine particles out of the force chains whereas the dilative response is mainly associated with the migration of fine particles into the force chains. In an assembly of coarse and fine particles, neither all of the fine particles nor all of the coarse ones participate in the force chains to carry the external loads, and therefore a more reasonable definition for equivalent skeleton void ratio is put forward in which a new parameter d is introduced to take into account the fraction of coarse particles absent from the force chains.

Keywords: silty sand; equivalent skeleton void ratio; fine particles; force chain; anisotropy; discrete element method

1. Introduction

Most liquefaction failures in geotechnical engineering practice (Ishihara 1993, Yang and Wei 2012), either under monotonic or cyclic loading conditions, are associated with silty sand that is comprised of coarse sand grains and some amount of fines at silt size (typically below 0.074mm in diameter). Due to the presence of fine particles, the mechanical behavior of sand becomes highly complex (Kuerbis *et al.* 1988, Georgiannou *et al.* 1990, Pitman *et al.* 1994, Yamamuro and Lade 1997, Lade and Yamamuro 1997, Zlatović and Ishihara 1997, Yamamuro and Lade 1999, Thevanayagam and Mohan 2000, Polito and Martin II 2001, Carraro *et al.* 2003, Ni *et al.* 2004, Murthy *et al.* 2007, Bobei *et al.* 2009, Monkul 2013, Rahman *et al.* 2014, Hsiao and Phan 2014, Vahidi-Nia *et al.* 2015, Chang *et al.* 2017, Hyodo *et al.* 2017, Patil *et al.* 2017, Porcino and Diano 2017). Several experimental studies on silty sand showed that the critical state soil mechanics (CSSM) theory that works for clean sand does not seem to work well for silty sand. For example, Yamamuro and Lade (1997) revealed that at a given fines content, the undrained shear responses of silty sands show increasing dilation with increasing confining pressure at a low pressure level, which is in contrast to the anticipated behavior of clean sand according to the CSSM theory. In the literature, this shear behavior has been referred to as a reverse behavior

(Yamamuro and Lade 1997). The test results of Thevanayagam and Mohan (2000) showed that this reverse behavior also takes place at relatively high confining pressures for sand-fines mixtures. Note that increasing confining pressure suppresses the dilatancy for clean sands. Such observations suggest that confining pressure may not be a fundamental cause resulting in the reverse behavior, but fines are assumed to play a role.

Several researchers have made attempts to study such reverse behavior within the framework of CSSM, attributing the malfunction of the CSSM theory to that the global void ratio e was not able to account for the role of fines in silty sand (e.g., Mitchell 1976, Kuerbis *et al.* 1988, Pitman *et al.* 1994, Thevanayagam and Mohan 2000, Thevanayagam and Mohan 2002). The hypothesis behind this argument is that not all fine particles in a silty sand specimen participate in the soil skeleton to sustain external forces, but rather, some of the fines are confined in voids, making no contribution to the force chains. An alternative index, known as skeleton void ratio e_s , was then put forward to describe the shear behavior of silty sand by treating all fine particles as voids (Mitchell 1976, Kenney 1977, Kuerbis *et al.* 1988, Georgiannou *et al.* 1990, Pitman *et al.* 1994, Thevanayagam and Mohan 2000, Polito and Martin II 2001, Carraro *et al.* 2003). This index was further revised as the so-called equivalent skeleton void ratio e_{se} , as expressed in Eq. (1), by treating only the fine particles not present in the force chains as the voids (Ni *et al.* 2004, Thevanayagam *et al.* 2002)

$$e_{se} = \frac{e + (1-b)fc}{1 - (1-b)fc} \quad (1)$$

where e is the global void ratio; fc is the fines content; b

*Corresponding author, Ph.D.

E-mail: beibing_dai@yahoo.com or daiib@mail.sysu.edu.cn

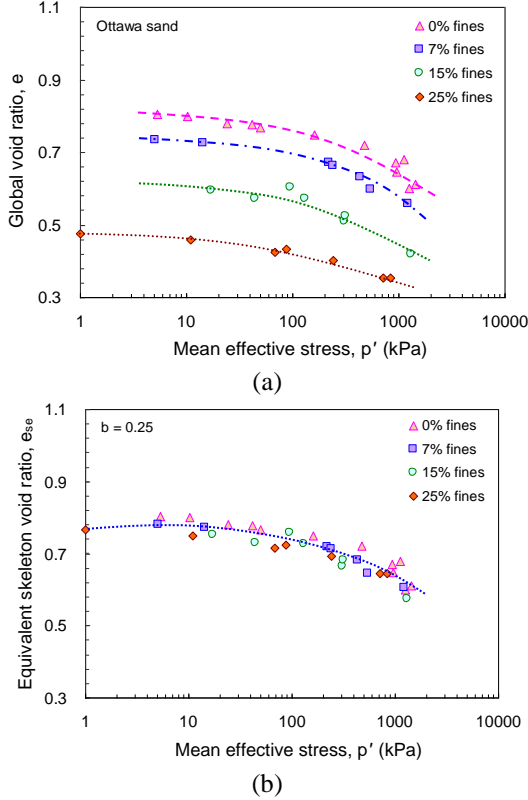


Fig. 1 (a) Critical state points in e - $\log p'$ space for Ottawa sand with different fines content and (b) a unique critical state line in e_{se} - $\log p'$ space with b assigned to be 0.25 (after Thevanayagam *et al.* 2002)

denotes the portion of fine particles participating in force chains. It was hypothesized (Ni *et al.* 2004, Thevanayagam *et al.* 2002, Yang *et al.* 2006, Rahman *et al.* 2008, Vahidinia *et al.* 2015) that with a properly assigned b value, a unique critical state locus (CSL) could be achieved through the best-fitting method for both clean sand and the sand mixed with fines in the e_{se} - $\log p'$ space, as shown in Fig. 1 for Ottawa sand having different fines content.

With the use of equivalent skeleton void ratio, a number of researchers (e.g., Thevanayagam *et al.* 2002, Ni *et al.* 2004, Yang *et al.* 2006, Rahman *et al.* 2008, Mohammadi and Qadimi 2015) have successfully captured the mechanical behavior of sands with various fines content in the CSSM framework. Moreover, Rahman *et al.* (2014) and Lashkari (2014) established the constitutive relations to predict the behavior of sands with fines, on the basis of the concept of equivalent skeleton void ratio and the corresponding modified state parameter in the CSSM theories. Also, Chang and Yin (2011) proposed a micromechanical model in the framework of CSSM to describe the mechanical behavior of sand-fines mixture, by identifying the critical state friction angle and critical state void ratio as a function of fines content to achieve a unique critical state line.

While the equivalent skeleton void ratio appears to be a useful index, the physical meaning of the parameter b is not yet well understood. As stated by Thevanayagam *et al.* (2002), b values should range from 0 to 1: “ $b = 0$ ” means that none of the fine particles are effective in force chains,

and “ $b = 1$ ” means that all of the fine particles are actively involved in force chains. The range of b values was further extended to include negative values for sands with plastic fines (Ni *et al.* 2004). This extension, however, does not follow the original physical meaning. Recently, Rahman *et al.* (2008) attempted to make b a predictable parameter by proposing an empirical equation as follows

$$b = \left\{ 1 - \exp \left[-m (f_c)^2 / k \right] \right\} (rf_c / f_{thre})^r \quad (2)$$

where f_c and f_{thre} are, respectively, the fines content and its threshold value separating sand-dominated soils and fines-dominated soils; r is the size ratio defined as d_{50}/D_{10} , where d_{50} is the particle size at 50% passing on the cumulative distribution curve of fine particles and D_{10} is the particle size at 10% passing on the cumulative distribution curve of coarse sand grains; k is expressed as $(1-r)^{0.25}$; m is a fitting constant. It is seen from Eq. (2) that the effect of basic particle attributes (e.g., particle shape) on b value has been ignored, but particle shape has been proved to be an essential factor influencing b through experimental observations (Yang *et al.* 2015).

In the literature the parameter b has been regarded as a constant relating only to the inherent attributes of silty sand, such as fines content and particle gradation. In the authors' view, however, the parameter b is a state-dependent variable which varies during shear and, especially, is affected by the confining pressure and packing density. To make the point, take a silty sand specimen that is liquefiable for example: The b value at an idealized liquefied state (i.e., the flow-type failure which means that soil flows like a liquid) with all particles having almost lost their contacts should be nearly zero, whereas it is a nonnegligible non-zero value at the state prior to undrained shearing (i.e., at the end of consolidation). The important implication here is that the b value as well as the role of fine particles should evolve during shear. In this context, such factors as confining pressure and void ratio can affect the participation of fine particles in force chains, and accordingly affect the b value.

Also, it is worth noting that, in a silty sand specimen subjected to loading, neither all of the coarse grains nor all of the fine grains will participate in the force chains. In this connection, in addition to fine grains, some coarse grains may also be ineffective ones in the soil skeleton and make no contribution to force transferring. From the perspective of micromechanics, it is important to consider the absence of both coarse and fine grains from the force chains. Hence a new parameter, d , representing the mass fraction of the coarse grains in the force chains (i.e., the ratio of the mass of coarse particles over the total mass of coarse particles in an assembly), is introduced into the expression of e_{se} in Eq. (1), giving a more rational definition for the equivalent skeleton void ratio

$$e_{se} = \frac{e + (1-b)fc + (1-d)(1-fc)}{1 - (1-b)fc - (1-d)(1-fc)} \quad (3)$$

where both d and b vary between 0 and 1. The parameter b in Eq. (3) has the same meaning as that in Eq. (1), denoting the proportion of the mass of fine particles in the total mass of fine particles.

To develop a better understanding of the physical meanings of the parameters b and d and the role of fines in the complicated behavior of silty sand, a series of numerical simulations have been conducted using the discrete element method (DEM). Compared with the real laboratory experiments, the DEM simulations have unique advantages in that they can offer concrete information on the inter-particle contacts and particle movements, which is crucial to understanding the role of the fine and course particles in a granular assembly and thus to clarifying the physical meaning of the equivalent skeleton void ratio. This paper presents the main results and findings from these simulations.

2. Numerical modeling

The discrete element method, initiated by Cundall (1971), has now evolved as a useful computational tool to study the mechanical behavior of granular materials (Rothenburg and Bathurst 1989, Thornton 2000, Bolton *et al.* 2008, Yimsiri and Soga 2010, Yan and Zhang 2013, Qian *et al.* 2013, Gu *et al.* 2014, Ma *et al.* 2014, Dai *et al.* 2015, Xu *et al.* 2015, Zhou *et al.* 2017). The program PFC2D (2005) was used in this study to conduct biaxial test simulations under the constant volume condition (i.e., the undrained condition in geotechnical laboratory tests). To allow for the irregularity of real particle shape, non-circular particles were used in this study. Each particle was formed by two circular constituent particles clumped together (see Fig. 2), and the two constituent particles were not allowed to break apart during loading. The aspect ratio of clumped particles was assigned to be 0.6, and the size of a clumped particle was described by an equivalent particle diameter (Dai *et al.* 2017). The built-in linear elastic contact model in PFC2D was used to describe the contact behavior between particles and the friction behavior at contacts was assumed to obey the Coulomb friction law.

Three particle gradations were considered in this study. The gradations A and B were generated by the addition of fines at different quantities, on the basis of the base gradation (i.e., gradation C). The base grading curve and fines grading curve are given in Fig. 2. For the fines and base grading curves, the mean particle sizes (d_{50}) are 0.058 mm and 0.54 mm, respectively, and the coefficients of uniformity (d_{60}/d_{10}) are 2.35 and 1.6, respectively. The fines content is about 2% and 1%, respectively, for the gradations A and B. With such fines content, the DEM simulations in this study have been proved to be to some extent able to capture the main characteristics of shear behaviors observed in triaxial tests. This is probably because the packing of assemblies in a 2D case is different from that in a 3D case, and thus the reproduction of the behaviors observed in a triaxial test may not require the same void ratio and fines content in a 2D simulation.

The gravitational deposition was used as the sample preparation method. As illustrated in Fig. 3, particles were firstly generated with arbitrary orientations in a designated domain. Subsequently, gravitational forces were enforced onto all particles by introducing a gravitational field, and thus the particles were deposited onto the bottom wall. At

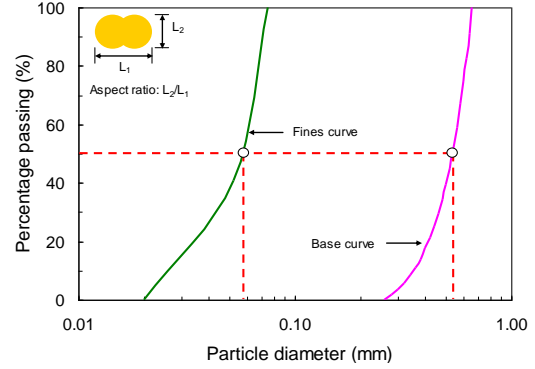


Fig. 2 Particle shape and size distribution used in numerical simulations

Table 1 Sample information

Test Name	Particle Gradation	Fines content (%)	Global Void Ratio, e	Particle Number, N	Confining Pressure, p (kPa)
TP-1	A	2	0.217	9057	200
TP-2	A	2	0.217	9013	800
TP-3	A	2	0.217	9034	1200
TD-4	B	1	0.216	5236	1000
TD-5	B	1	0.228	5147	1000
TD-6	B	1	0.235	5115	1000
TG-7	A	2	0.216	9013	1000
TG-8	B	1	0.217	5212	1000
TG-9	C	0	0.217	2881	1000

Table 2 Modeling parameters

Parameters	Value
Particle Density, ρ	2.65 g/cm ³
Aspect Ratio, R_a	0.6
Inter-particle Friction, μ_s	0.5
Wall Friction, μ_w	0.5
Normal & Tangential Stiffness, k_n & k_s	10 ⁹ N/m
Wall Stiffness, k_w	10 ⁹ N/m
Damping Factor, α	0.7

the end of deposition, an area of $25 \times 25 \text{ mm}^2$ was chosen to be the final specimen, and then compaction was performed with the four rigid boundary walls simultaneously moving inward to consolidate the specimen towards a target confining stress. The undrained shearing was carried out by moving the two loading walls in the strain-controlled mode and meanwhile maintaining the sample volume/area constant. The loading rate is set to be $\Delta \varepsilon_a = 8.0 \times 10^{-8} / \text{step}$, and the quasi-static shear was guaranteed with a cycling requirement specified in the simulation, which refers to an upper limit for the ratio between the maximum unbalanced force and the average contact force (1% in this study) (Dai and Yang 2017). During shear, the gravity of particles was removed and the local damping was activated with the default value of 0.7. The applied stress was estimated by averaging the particle-wall contact forces, and the applied strain was given as $\varepsilon_a = \Delta L/L$, in which ΔL is the

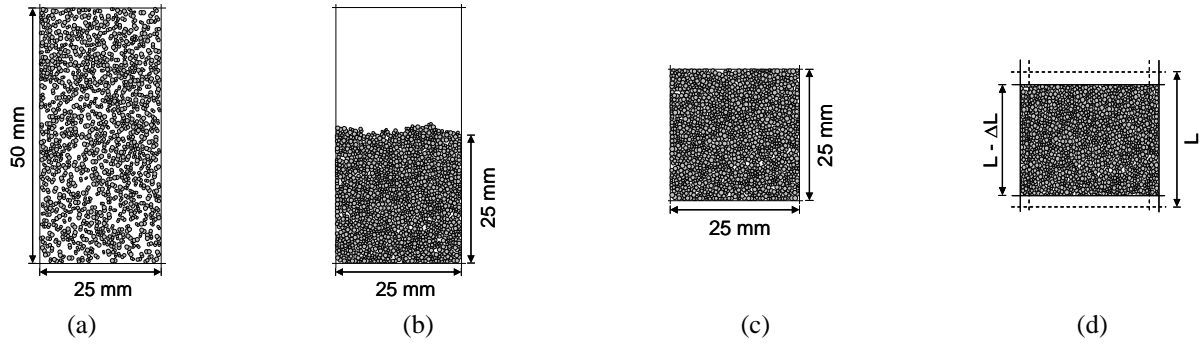


Fig. 3 Sample preparation and shearing: (a) initial particles distribution, (b) deposition completed, (c) final specimen and (d) shearing of a sample

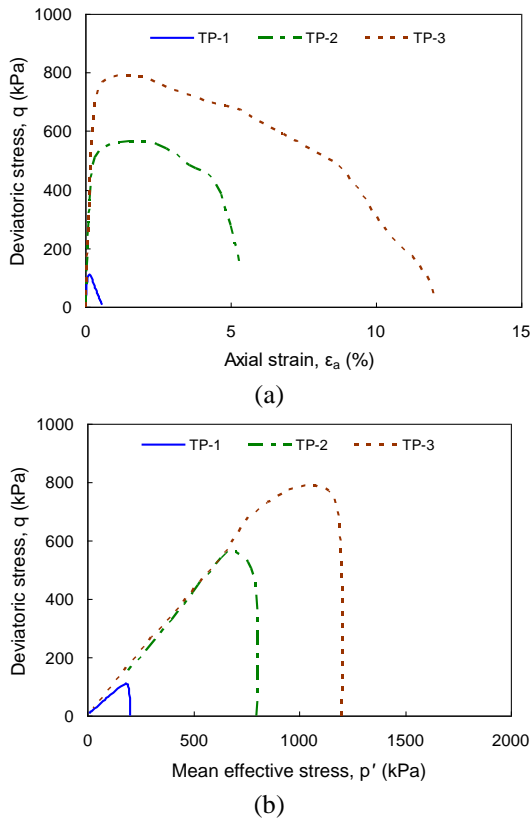


Fig. 4 Shear behaviors of the specimens TP-1, TP-2 and TP-3

displacement of loading walls and L is the original height of confining walls (see Fig. 3(d)). In total 9 specimens were generated in this study for the simulations of biaxial shear test, and they were categorized into three groups possessing respectively different confining pressures (TP series), packing densities (TD series) and particle gradations (TG series). A summary of the numerical test series and modeling parameters is listed in Tables 1 and 2.

In order to make meaningful comparisons in this study, fine particles are differentiated from coarse particles using the reference particle size $R_s = 0.04$ mm in radius ($\approx 0.074/2$ mm). In determining the values of b and d , the following rule has been used: particles with zero contact forces are regarded as ineffective, that is, they are considered to be absent from the force chains. On the basis of this criterion, the fine and coarse particles in and out of force chains can

be easily identified in a DEM test, such that the statistics of the quantities of these particles can be made to evaluate the b and d values according to their physical definitions. With the b and d values at various shear strain levels, the evolutions of b and d can be obtained.

3. Results and discussions

3.1 Shear behavior of specimens under different confining pressures

The test series of TP-1 to TP-3 were conducted to investigate the influence of confining pressure on the overall shear responses and associated variations of the parameters b and d during the loading process. Fig. 4 compares the stress-strain behaviors and stress paths of the three specimens. Fig. 5 gives the variations of the parameters b and d for the specimens TP-1 and TP-3.

It is clear that all specimens undergo complete liquefaction with almost zero strength at the end of the test and that both b and d values decrease monotonically with the axial strain. The parameter b is not a constant as assumed in the literature, but rather it varies during the loading process. The decrease of parameters b and d indicates a continuous movement of fine and coarse particles out of the force chains during shear, and this is congruous with the macroscopic liquefaction behavior.

It is worth noting that the strain level developed in the specimen TP-3 (at 1200 kPa) is much higher than that developed in the specimen TP-1 (at 200 kPa) and the peak stress ratio (q/p') achieved by TP-3 (0.764) is also larger than that of TP-1 (0.601). These observations suggest that at a similar void ratio, the specimen under a higher confining pressure (TP-3) is less contractive than the specimen at a lower confining pressure (TP-1). This finding is in agreement with the so-called reverse behavior observed by Yamamuro and Lade (1997) in their laboratory testing on a silty sand.

To explain the reverse behavior, Yamamuro and Lade (1997) hypothesized that in the course of isotropic compression, a higher consolidation pressure can move fine particles between coarse grains into the voids more easily and create more contacts between large particles, thus giving a stiffer, less compressible soil skeleton. However, the variations of b and d values in Fig. 5 suggest a different

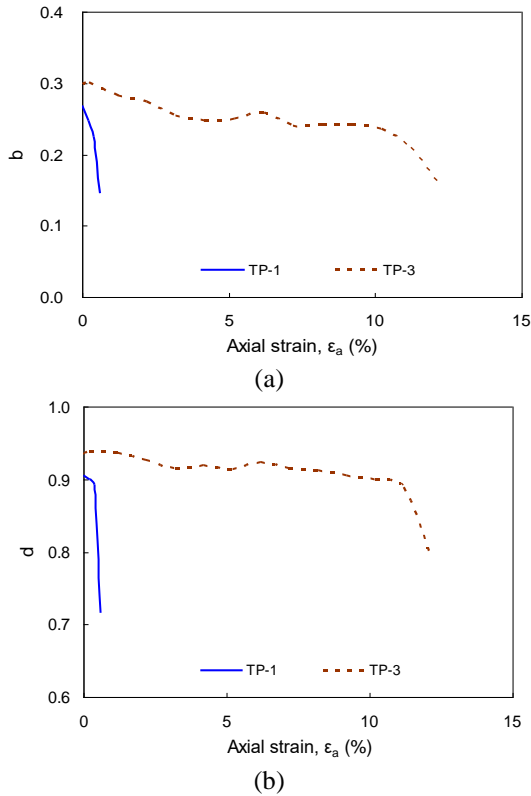


Fig. 5 Variations of b and d values for the specimens TP-1 and TP-3

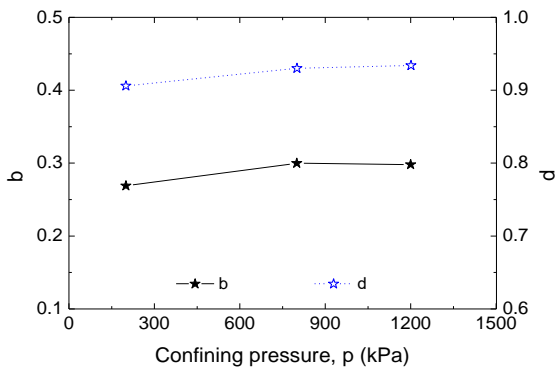


Fig. 6 Relations of b and d values at the initial state with confining pressure (test series TP-1 to TP-3)

mechanism: Both b and d values of the specimen TP-3 at the initial state are larger than those of TP-1, meaning that the consolidation under a higher confining pressure allows more particles (both fine and coarse ones) to participate in the force chains to carry the external load and hence contributes to a stiffer soil skeleton. In this regard, it is the movement of both fine and coarse particles into the force chains that is primarily responsible for the decrease of contraction potential, instead of the removal of fine particles out of the force chains as hypothesized (Yamamuro and Lade 1997).

Fig. 6 shows the variations of b and d values at the state prior to shearing, with the confining pressure for the three specimens TP-1, TP-2 and TP-3. Both b and d values are found to basically increase with confining pressure, suggesting that more particles (both fine and coarse ones)

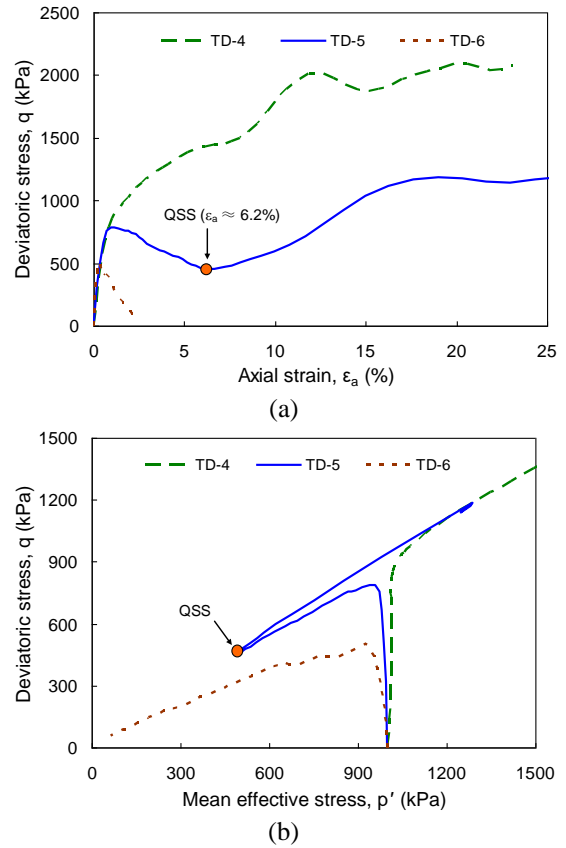


Fig. 7 Shear behaviors of the specimens TD-4, TD-5 and TD-6

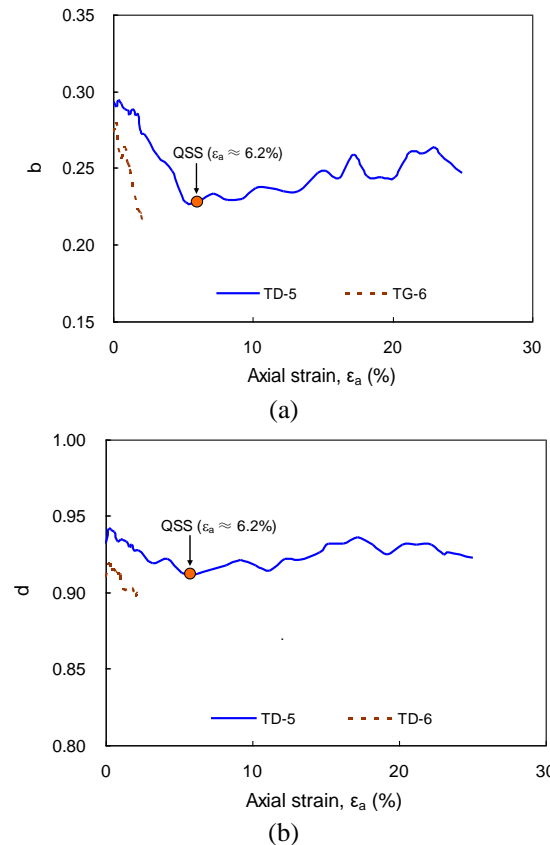


Fig. 8 Variations of b and d values for the specimens TD-5 and TD-6

will be brought into force chains with increasing confining pressure. This trend is in support of the mechanism proposed above.

3.2 Shear behavior of specimens under different packing densities

Fig. 7 depicts the macroscopic shear behaviors of three specimens (TD-4, TD-5 and TD-6) which were packed at different densities but subjected to the same confining pressure. The specimen TD-4 demonstrates the most dilatative behavior. The relatively loose specimen TD-5 shows a dilatant response after undergoing a contractive response at the initial loading stage, with the so-called quasi-steady state (QSS) (Ishihara 1993, Yang and Dai 2011) taking place at the strain level of about 6.2%. The loosest specimen TD-6 exhibits a complete contractive response. It should be noted that the concepts of contraction and dilation do not refer to a real volume change of specimens in this study. The equivalent skeleton void ratio cannot be taken as an index for a direct measurement of contraction (or dilation), despite that its variation is related to the contraction (or dilation) behavior.

The values of b and d for the two specimens are plotted against shear strain in Fig. 8. Interestingly, the b values of TD-5 experience a drop prior to the occurrence of the QSS state, and then rise with further shearing. In Fig. 8(b), the d values show an evolution trend similar to the b values, which suggests a similar migrating mechanism in the soil skeleton for coarse particles. However, the variation of d appears to be less significant than that for b , implying that fine particles tend to undergo more movements than coarse particles during shear and the macroscopic responses are controlled more by the movement of fine particles. According to the physical meaning of the parameter b , the temporary decrease of b values means that some fine particles quit from the force chains, giving rise to the macroscopically observed contractive response at the initial stage of shearing. The increase of b after this initial stage means that some fine particles move back into the force chains, yielding a stiffer soil skeleton and a more dilatative response.

Compared with TD-5, both b and d values of TD-6 decrease continuously with axial strain. This implies that the liquefaction of this specimen is due to the loss of contacts of both fine and coarse particles. At the initial state prior to shearing, both b and d values of TD-5 are larger than the corresponding ones of TD-6, indicating that there exists a higher participation degree in the force chains for fine and coarse particles of TD-5. This finding is considered reasonable because a decrease of global void ratio allows more particles to move into the force chains to form contacts and thus enhances the stiffness of soil skeleton. This consideration is supported by the variations of initial b and d values with the global void ratio as shown in Fig. 9.

3.3 Shear behavior of specimens with different particle gradations

Fig. 10 compares the shear behaviors of the three specimens TG-7, TG-8 and TG-9 under the same packing

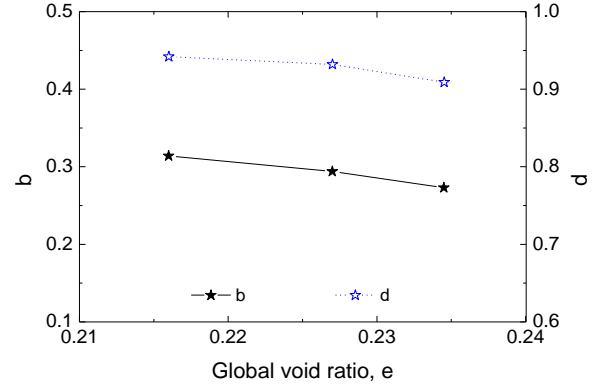


Fig. 9 Relations of b and d values at the initial state with global void ratio (test series TD-4 to TD-6)

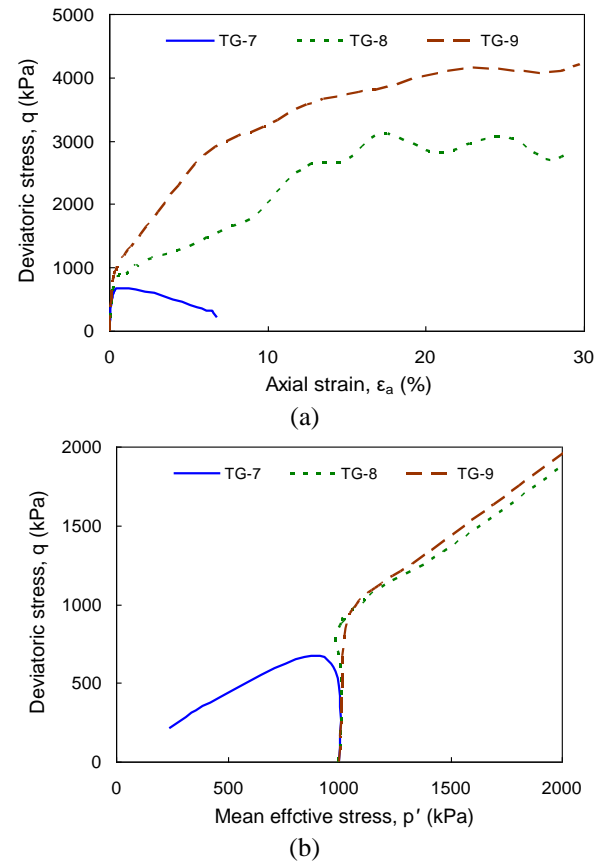


Fig. 10 Shear behaviors of the specimens TG-7, TG-8 and TG-9

density and consolidation pressure but with different particle gradations. The specimen TG-7 has the highest content of fine particles and exhibits a highly contractive response and the specimen TG-9 with no fines exhibits the most dilatative response. The discrepancies of the behaviors indicate that the contractiveness of an assembly of fine and coarse particles increases with increasing content of fines particles. This result is in good agreement with the observations from laboratory experiments, for example, Yamamuro and Lade (1997), Thevanayagam and Mohan (2000), Yang and Wei (2012) and Yang *et al.* (2015), as shown in Fig. 11. The mechanism behind the observation is that increasing fines content abates the contribution of

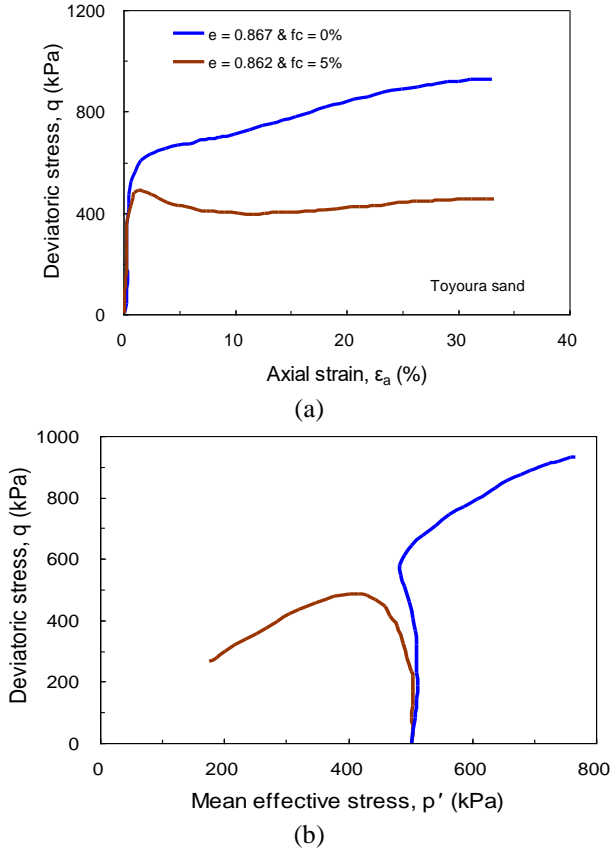


Fig. 11 Laboratory test findings of Yang and Wei (2012)

coarse particles in the soil skeleton, and thus causes a more contractive and weaker soil structure with more fine particles being trapped in the void space. In this regard, the b values, as evidenced by Table 3, decrease with increasing fines content.

It is worth noting that the decrease of b values with increasing fines content does not suggest that the absolute quantity of fine particles in force chains should be reduced. Rather, the number of fine particles in force chains (N_i) is found to increase as fines content increases (see Table 3). This is understandable because the total number of fine particles will increase with the increase of fines content and more fine particles are desired to participate in the force chains, but this does not mean that the ratio of fine particles in force chains (i.e., the b value) must increase correspondingly. At a given global void ratio and a given confining pressure, the increase of fine particles in the force chains means that there are more opportunities for fine particles to locate at or near the contacts between coarse particles. These fine particles may induce a greasing effect which makes the assembly more contractive, since they are prone to rolling against the coarse particles. This is considered to be another possible mechanism for the observed increase in contractiveness with increasing content of fine particles.

To better the understanding, Fig. 12 gives the evolutions of b and d for specimens TG-7 and TG-8. The liquefied TG-7 exhibits a decrease in both b and d values during shear. The implication is that fine particles are continuously removed from the force chains and the loss of supporting

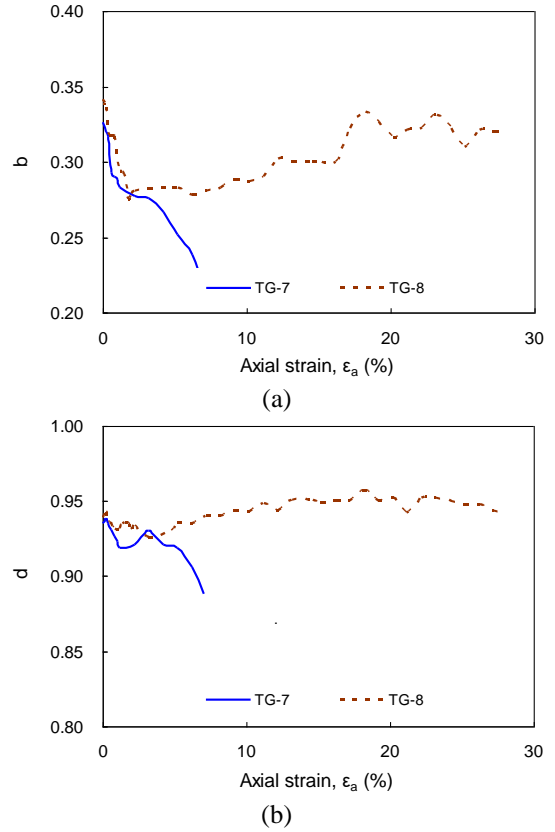


Fig. 12 Variations of b and d values for the specimens TG-7 and TG-8

Table 3 Parameters b , d , N_i and N_o at the initial state

Test Name	Particle Gradation	b	d	Particle Number	
				N_i^*	N_o^*
TG-7	A	0.320	0.935	1162	3503
TG-8	B	0.341	0.939	379	1209

* N_i – number of fine particles in force chains; N_o – number of fine particles in voids

effect from fine particles induces the removal of coarse particles out of the force chains as well, leading to complete liquefaction. By comparison, the initial decrease of b values for TG-8 signifies a temporary contractive response that is caused by fine particles moving out of the force chains; the subsequent increase of b values corresponds to the dilative response which is associated with fine particles migrating back into the force chains. Similarly, the d values of TG-8 experience a temporary drop at first and then an increase with further shearing. Note that the variation of d is less significant than that of b . This suggests that the macroscopic response of TG-8 is mainly associated with the movement of fine particles.

4. Comparison of equivalent skeleton void ratio with different definitions

By focusing on the three specimens with different confining pressures (TP-1 to TP-3), Fig. 13(a) shows a

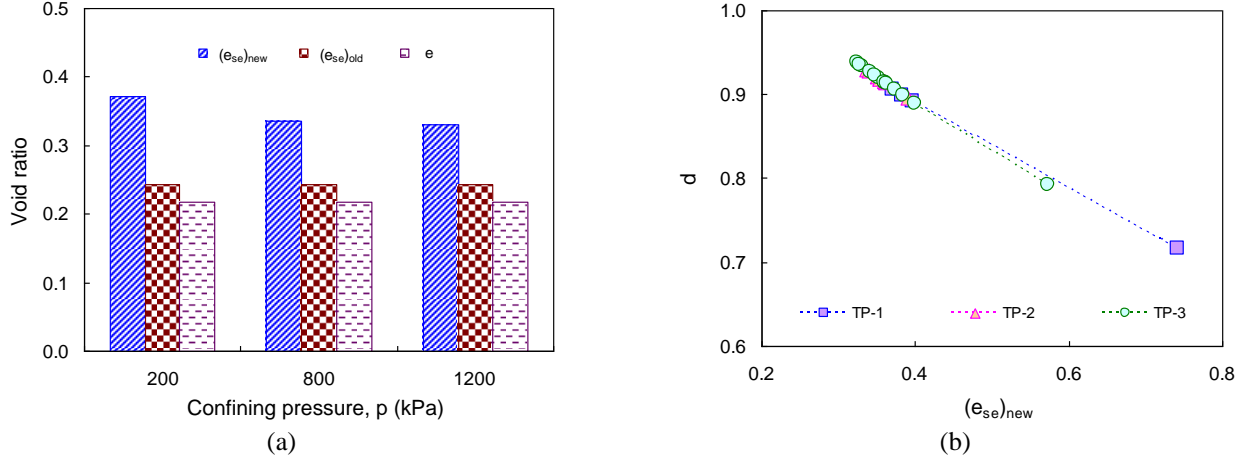


Fig. 13 (a) Comparison of two definitions of equivalent skeleton void ratio at the initial state and (b) relationship between the parameter d and the newly defined equivalent skeleton void ratio during shear

comparison of the two definitions of equivalent skeleton void ratio: the existing definition of equivalent skeleton void ratio in Eq. (1), denoted as $(e_{se})_{old}$, and the new one as proposed in Eq. (3), which is denoted as $(e_{se})_{new}$. It is seen that in the concerned range of confining pressure, $(e_{se})_{old}$ is well below $(e_{se})_{new}$ and is almost a constant. The striking discrepancies between $(e_{se})_{old}$ and $(e_{se})_{new}$ suggest that there are some amount of coarse particles not present in force chains and having no contribution to force transferring in the soil skeleton. The non-dependence of equivalent skeleton void ratio $(e_{se})_{old}$ on confining pressure is due probably to that the volume (or area) of small particles is so small that the movement of small particles into or out of force chains under various consolidation pressures is unable to induce notable variations in void space, despite that the b values, as indicated by Fig. 6, are shown to rely on confining pressure. It is also noted that the traditional global void ratio e is slightly smaller than $(e_{se})_{old}$, due to the effect of parameter b . In addition, Fig. 13(b) shows a good correlation between the d value and the newly defined equivalent skeleton void ratio $(e_{se})_{new}$.

5. Micromechanical consideration

Coordination number (CN), which refers to the average contact number per particle, is a useful index characterizing the packing state of a granular assembly. Thornton (2000) proposed a so-called mechanical coordination number (CN) by excluding the particles having no contribution to the force transfer. For mixtures of coarse and fine particles, Yang *et al.* (2015) provided experimental evidence for the existence of different types of contacts, such as large particle-to-large particle contacts (Type I contact in Fig. 14), small particle-to-large particle contacts (Type II contact in Fig. 14), and small particle-to-small particle contacts (Type III contact in Fig. 14). They hypothesized that the macroscopic behavior is highly associated with the proportions of such contacts. In line with this consideration, the mechanical coordination number (overall CN) is decomposed into three components in this study: (1) coordination number contributed by contacts between large

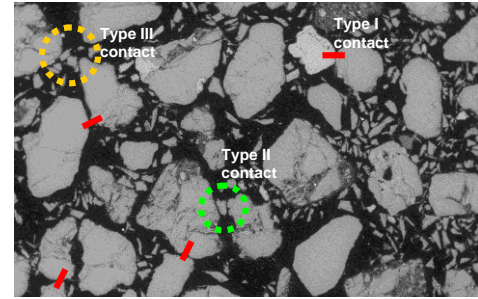


Fig. 14 A microscopic view of different types of contacts in silty sand (after Yang *et al.* 2015)

particles (i.e., the ratio between the number of L-L contacts and the total number of particles), noted as L-L coordination number or L-L CN (CN_{L-L}); (2) coordination number contributed by contacts between small particles (i.e., the ratio between the number of S-S contacts and the total number of particles), noted as S-S coordination number or S-S CN (CN_{S-S}); (3) coordination number contributed by contacts formed between large and small particles (i.e., the ratio between the number of S-L contacts and the total number of particles), noted as S-L coordination number or S-L CN (CN_{S-L}).

For the liquefied specimen TP-3, Fig. 15 shows the evolutions of the four coordination numbers during shear. The overall CN decreases as shearing goes on, reaching 3.2 at the end of the test. The S-S CN also undergoes a slight decrease during shear. Similarly, the L-L CN does not vary significantly before the strain level arrives at 10%, but after that it suffers from a notable decrease. Apparently, the variation of the S-L CN exhibits a very similar manner as that of the overall CN . A dramatic drop of the S-L CN takes place in the final stage of shear. The evolution of S-L CN signifies that fine particles persistently quit from the force chains upon shear. This is consistent with the finding on the evolution of b values in Fig. 5. The above observations suggest that the variation of overall CN depends to a great extent on the variation of S-L CN and that the continuous loss of S-L contacts is the primary cause responsible for the decrease of overall CN .

Based on the observations on the evolutions of

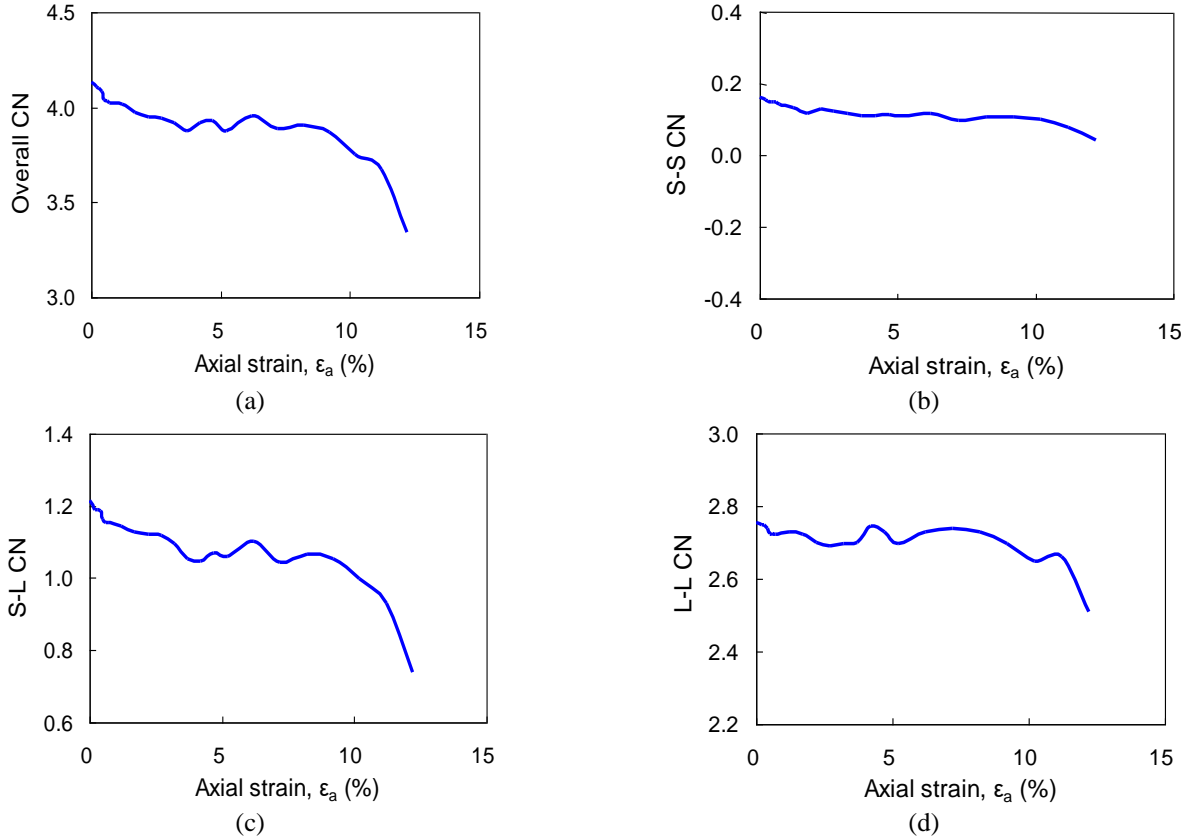


Fig. 15 Variation of coordination number (CN) with axial strain for the specimen TP-3

coordination numbers, the liquefaction mechanism of the specimen TP-3 is given as follows. At the initial stage of shearing, some fine particles are dislodged into voids (see Figs. 5(a) and 15(c)), rendering a relatively soft soil skeleton; but the movement of these fine particles into voids does not create more contacts between coarse particles (see Fig. 15d), rather, some coarse particles in contact with fine particles may also be removed from the force chains due to the loss of the supporting effect from the fine particles (see Fig. 5b), hence promoting the liquefaction potential. As shearing goes on, more and more particles (both fine and coarse ones) are displaced into voids, inducing a much softer soil skeleton and eventually a fully liquefied state.

Fig. 16 gives the evolutions of the four coordination numbers during shear for the non-liquefied specimen TG-8. It is shown that the S-L CN and S-S CN dominate the variation of the overall coordination number, suggesting that fine particles play an essential role in the shear responses of the specimen TG-8. The temporary decrease of the S-L CN and S-S CN, which matches the interim macroscopic contractive response, signifies the removal of some fine particles from the soil skeleton, and their regain with further shearing means that a number of fine particles move back into the soil skeleton and strengthen it, rendering a dilative shear response. This shearing mechanism is consistent with that revealed from the variations of b and d values in Fig. 12.

Rothenburg and Bathurst (1989) put forward the following functions $f(\phi)$ and $E(\phi)$ to characterize the angular variations of the contact normal force intensity and

distribution probability of contact unit normal vectors

$$f(\phi) = f_0 \{1 + a_f \cos 2(\phi - \phi_f)\} \quad (4)$$

$$E(\phi) = E_0 \{1 + a_n \cos 2(\phi - \phi_n)\} \quad (5)$$

where f_0 is the measure of average contact normal force; a_f gives the anisotropy magnitude for the angular distribution of contact normal forces; ϕ_f denotes the principal anisotropy direction; the parameters a_n and ϕ_n define the fabric anisotropy magnitude and principal anisotropy direction in terms of contact unit normal vectors. Effort is made here to determine for the specimens TP-3 and TG-8 the values of f_0 , a_f and a_n for the contact forces and contact unit normal vectors at the three types of contacts and the overall contacts during the entire loading process. The results are given in Figs. 17 and 18. It is interesting to note that the anisotropy magnitude for the contact normal forces at the L-L contacts is higher than those at the S-S and S-L contacts. In particular, the anisotropy magnitude for the overall contacts is very close to that for the L-L contacts. Similar observations can be obtained for the mean contact normal forces (Figs. 17(b) and 18(b)). These results suggest that fine particles are mainly in the weak force chains whereas coarse particles are mainly in the strong force chains. This has explained why fine particles exhibit a higher degree of movement during loading.

Fig. 19 presents the evolutions of the anisotropy magnitude a_n in terms of contact unit normal vectors for the

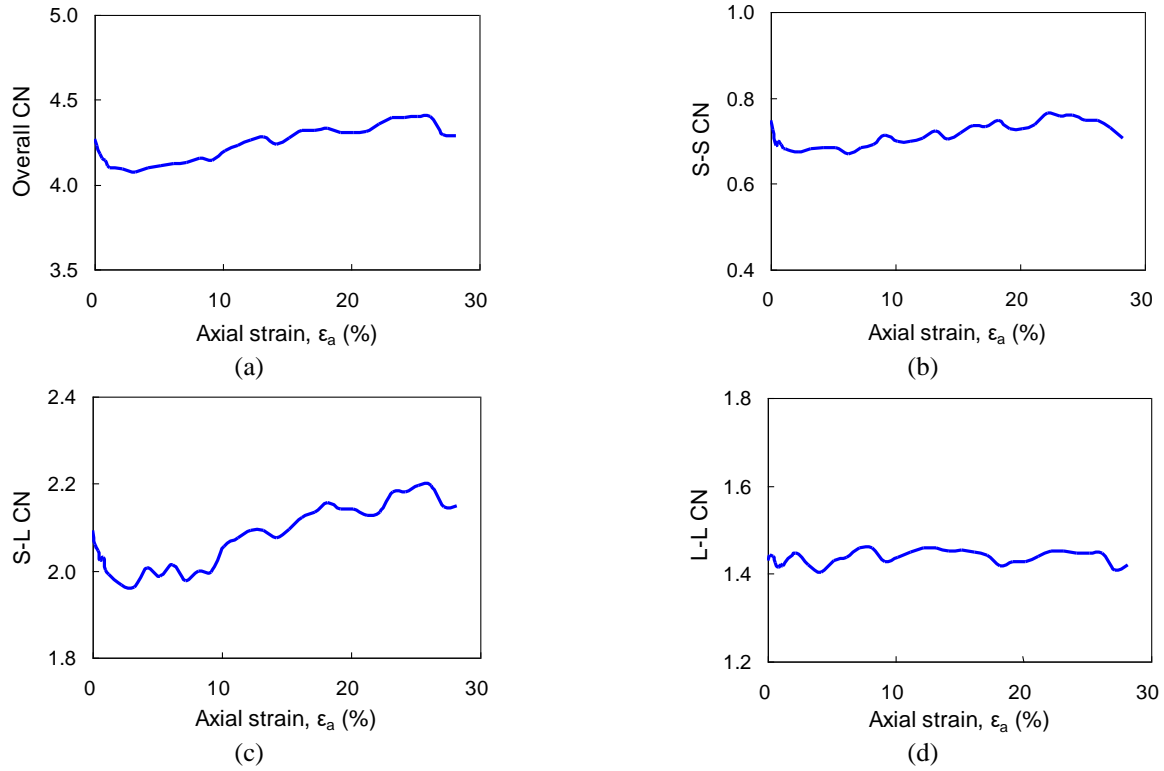


Fig. 16 Variation of coordination number (CN) with axial strain for the specimen TG-8

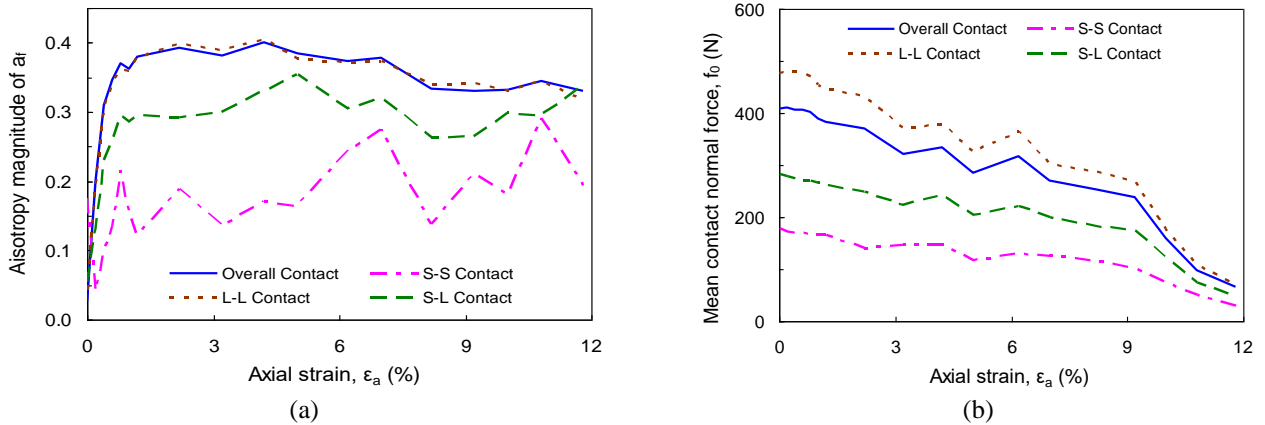


Fig. 17 Evolutions of (a) the force anisotropy magnitude a_f , and (b) mean contact normal force f_0 , for the specimen TP-3

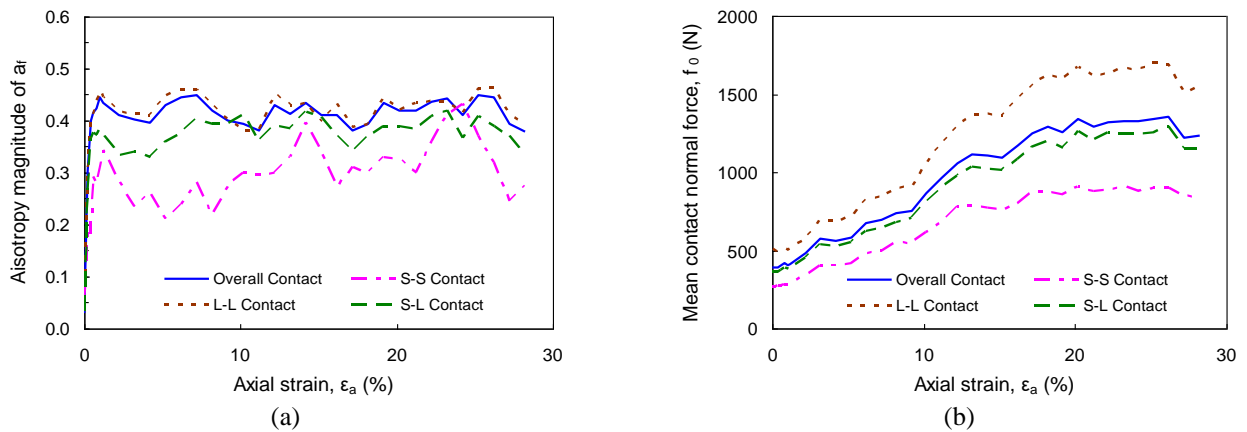


Fig. 18 Evolutions of (a) the force anisotropy magnitude a_f , and (b) mean contact normal force f_0 , for the specimen TG-8

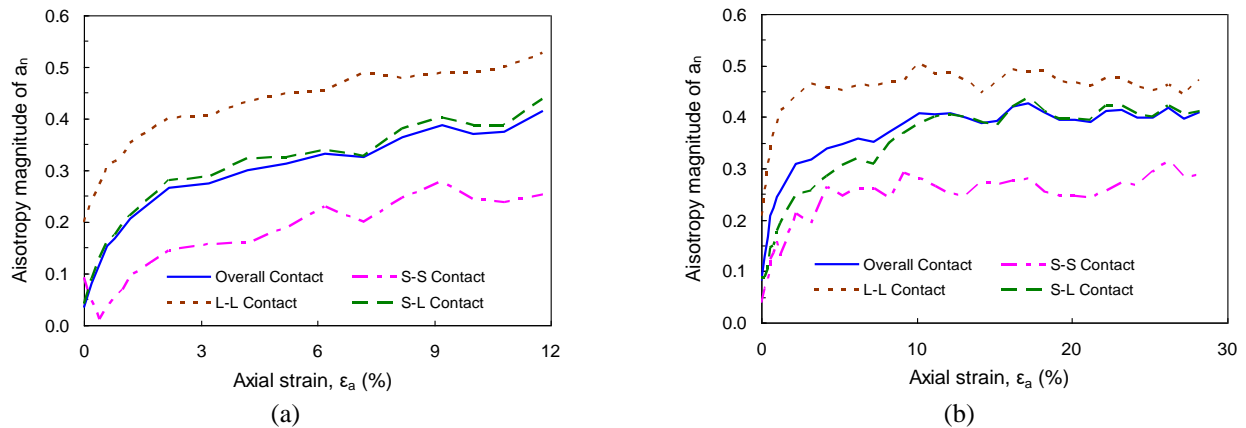


Fig. 19 Evolutions of the anisotropy magnitude a_n for the specimens of (a) TP-3 and (b) TG-8

specimens of TP-3 and TG-8. It can be seen that the anisotropy magnitudes at the L-L contacts are larger than those at the S-L and S-S contacts, which has further evidenced that fine particles are mainly in weak force chains and coarse particles are in strong force chains. Interestingly, the anisotropy magnitudes for the overall contacts are close to those for the S-L contacts for both specimens of TP-3 and TG-8.

6. Conclusions

This paper reports a DEM study on the shear behavior of assemblies composed of coarse and fine particles, with particular efforts made to discuss the concept of the equivalent skeleton void ratio that has been increasingly used in the literature to characterize the density of silty sand. The main findings are summarized as follows:

- In an assembly of coarse and fine particles, neither all of the fine particles nor all of the coarse particles will participate in the force chains. Therefore, in addition to the parameter b to allow for the participation of fine particles in the force chains, the current definition for the equivalent skeleton void ratio is modified by introducing a new parameter d to take into account the absence of coarse particles from the force chains.

- The assumption that the parameter b is a constant in the literature is inappropriate. This parameter is a state-dependent variable that varies with the consolidation pressure and packing density and evolves in the loading process. Similarly, the parameter d is not a constant but is state dependent.

- The macroscopically observed contractive response is mainly caused by the movement of fine particles out of the force chains, manifested by a decrease of the b value, whereas the dilative response is mainly associated with the migration of fine particles into the force chains, manifested by an increase of the b value.

- At a similar global void ratio, the assembly of coarse and fine particles under a higher confining pressure exhibits a less contractive response than the same assembly under a lower confining pressure. This reverse behavior is due probably to that the consolidation under a higher confining pressure allows more particles (both fine and coarse

particles) to take part in the force chains to carry the external load.

- In the assemblies of coarse and fine particles, fine particles are found to be mainly in the weak force chains whereas coarse particles are mainly in the strong force chains. Therefore, fine particles exhibit a higher degree of movement during loading than coarse particles. The movement of fine particles within the soil skeleton plays a crucial role in the overall macroscopic behavior.

Acknowledgements

The authors thank the financial support provided by the National Natural Science Foundation of China (No. 51209237; 41772283) and HKRGC under the General Research Fund scheme (Grant No. 17250316). The support from the Research Funds of Key Laboratory of Geotechnical and Underground Engineering of Ministry of Education (Tongji University) (No. KLE-TJGE-B1702) is also gratefully acknowledged.

References

- Bobei, D.C., Lo, S.R., Wanatowski, D., Gnanendran, C.T. and Rahman, M.M. (2009), "Modified state parameter for characterizing static liquefaction of sand with fines", *Can. Geotech. J.*, **46**(3), 281-295.
- Bolton, M.D., Nakata, Y. and Cheng, Y.P. (2008), "Micro- and Macro-mechanical behavior of DEM crushable materials", *Géotechnique*, **58**(6), 471-480.
- Carraro, J.A.H., Bandini, P. and Salgado, R. (2003), "Liquefaction resistance of clean and non-plastic silty sands based on cone penetration resistance", *J. Geotech. Geoenviron. Eng.*, **129**(11), 965-976.
- Chang, C.S. and Yin, Z.Y. (2011), "Micromechanical modeling for behavior of silty sand with influence of fine content", *Int. J. Solids Struct.*, **48**(19), 2655-2667.
- Chang, C.S., Meidani, M. and Deng, Y. (2017), "A comparison model for sand-silt mixtures based on the concept of active and inactive voids", *Acta Geotech.*, **12**(6), 1301-1317.
- Cundall, P.A. (1971), "A computer model for simulating progressive, large scale movements in blocky rock systems", *Proceedings of the International Symposium on Rock*

- Mechanics*, Nancy, France, October.
- Dai, B.B. and Yang, J. (2017), "On shear strength of assemblies of frictionless particles", *Int. J. Geomech.*, **17**(11), 04017102.
- Dai, B.B., Yang, J. and Luo, X. (2015), "A numerical analysis of the shear behavior of granular soil with fines", *Particuology*, **21**, 160-172.
- Dai, B.B., Yang, J. and Zhou, C.Y. (2017), "Micromechanical origin of angle of repose in granular materials", *Granul. Matter*, **19**(2), 24.
- Georgiannou, V.N., Burland, J.B. and Hight, H.W. (1990), "The undrained behavior of clayey sands in triaxial compression and extension", *Géotechnique*, **40**(3), 431-449.
- Gu, X.Q., Huang, M.S., and Qian, J.G. (2014), "DEM investigation on the evolution of microstructure in granular soils under shearing", *Granul. Matter*, **16**(1), 91-106.
- Hsiao, D.H. and Phan, V.T.A. (2014), "Effects of silt contents on the static and dynamic properties of sand-silt mixtures", *Geomech. Eng.*, **7**(3), 297-316.
- Hyodo, M., Wu, Y., Kajiyama, S., Nakata, Y. and Yoshimoto, N. (2017), "Effect of fines on the compression behaviour of poorly graded silica sand", *Geomech. Eng.*, **12**(1), 127-138.
- Ishihara, K. (1993), "Liquefaction and flow failure during earthquakes", *Géotechnique*, **43**(3), 351-415.
- Itasca. (2005), *User's Manual for PFC2D*, Itasca Consulting Group, Inc.
- Kenney, T.C. (1977), "Residual strengths of mineral mixtures", *Proceedings of the 9th International Conference on Soil Mechanics and Foundation Engineering*, Tokyo, Japan, July.
- Kuerbis, R.H., Negussey, D. and Vaid, Y.P. (1988), "Effect of gradation and fines content on the undrained response of sand", *Geotech. Special Publ.*, **21**, 330-345.
- Lade, P.V. and Yamamuro, J.A. (1997), "Effects of non-plastic fines on static liquefaction of sands", *Can. Geotech. J.*, **34**(6), 918-928.
- Lashkari, A. (2014), "Recommendations for extension and recalibration of an existing sand constitutive model taking into account varying non-plastic fines content", *Soil Dyn. Earthq. Eng.*, **61**, 212-238.
- Ma, G., Chang, X.L., Zhou, W. and Ng, T.T. (2014), "Mechanical response of rockfills in a simulated true triaxial test: A combined FDEM study" *Geomech. Eng.*, **7**(3), 317-333.
- Mitchell, J.K. (1976), *Fundamentals of Soil Behaviors*, Wiley, New York, U.S.A.
- Mohammadi, A. and Qadimi, A. (2015), "A simple critical state approach to predicting the cyclic and monotonic response of sands with different fines contents using the equivalent intergranular void ratio", *Acta Geotech.*, **10**(5), 587-606.
- Monkul, M.M. (2013), "Influence of gradation on shear strength and volume change behavior of silty sands", *Geomech. Eng.*, **5**(5), 401-417.
- Murthy, T.G., Loukidis, D., Carraro, J. A.H. and Salgado, R. (2007), "Undrained monotonic response of clean and silty sands", *Géotechnique*, **57**(3), 273-288.
- Ni, Q., Tan, T.S., Dasari, G.R. and Hight, D.W. (2004), "Contribution of fines to the compressive strength of mixed soils", *Géotechnique*, **54**(9), 561-569.
- Patil, U.D., Puppala, A.J., Hoyos, L.R. and Pedarla, A. (2017), "Modeling critical-state shear strength behavior of compacted silty sand via suction-controlled triaxial testing", *Eng. Geol.*, **231**, 21-33.
- Pitman, T.D., Robertson, P.K. and Segoo, D.C. (1994), "Influence of fines on the collapse of loose sands", *Can. Geotech. J.*, **31**(5), 728-739.
- Polito, C.P. and Martin II, J.R. (2001), "Effects of non-plastic fines on the liquefaction resistance of sands", *J. Geotech. Geoenviron. Eng.*, **127**(5), 408-415.
- Porcino, D.D. and Diano, V. (2017), "The influence of non-plastic fines on pore water pressure generation and undrained shear strength of sand-silt mixtures", *Soil Dyn. Earthq. Eng.*, **101**, 311-321.
- Qian, J.G., You, Z., Huang, M.S. and Gu, X.Q. (2013), "A micromechanics-based model for estimating localized failure with effects of fabric anisotropy", *Comput. Geotech.*, **50**, 90-100.
- Rahman, M., Lo, S. and Dafalias, Y. (2014), "Modelling the static liquefaction of sand with low-plasticity fines", *Géotechnique*, **64**(11), 881-894.
- Rahman, M.M., Lo, S.R. and Gnanendran C.T. (2008), "On equivalent granular void ratio and steady state behavior of loose sand with fines", *Can. Geotech. J.*, **45**(10), 1439-1456.
- Rothenburg, L. and Bathurst, R.J. (1989), "Analytical study of induced anisotropy in idealized granular materials", *Géotechnique*, **39**(4), 601-614.
- Thevanayagam, S. and Mohan, S. (2000), "Intergranular state variables and stress-strain behaviour of silty sands", *Géotechnique*, **50**(1), 1-23.
- Thevanayagam, S., Shenthan, T., Mohan, S. and Liang, J. (2002), "Undrained fragility of clean sands, silty sands and sandy silts", *J. Geotech. Geoenviron. Eng.*, **128**(10), 849-859.
- Thornton, C. (2000), "Numerical simulations of deviatoric shear deformation of granular media", *Géotechnique*, **47**(2), 319-329.
- Vahidi-Nia, F., Lashkari, A. and Binesh, S.M. (2015), "An insight into the mechanical behavior of binary granular soils", *Particuology*, **21**, 82-89.
- Xu, W.J., Li, C.Q. and Zhang, H.Y. (2015), "DEM analyses of the mechanical behavior of soil and soil-rock mixture via the 3D direct shear test", *Geomech. Eng.*, **9**(6), 815-827.
- Yamamuro, J.A. and Lade, P.V. (1997), "Static liquefaction of very loose sands", *Can. Geotech. J.*, **34**(6), 905-917.
- Yamamuro, J.A. and Lade, P.V. (1999), "Experiments and modelling of silty sands susceptible to static liquefaction", *Mech. Cohes. Frict. Mater. Struct.*, **4**(6), 545-564.
- Yan, W. and Zhang, L. (2013), "Fabric and the critical state of idealized granular assemblages subject to biaxial shear", *Comput. Geotech.*, **49**, 43-52.
- Yang, J. and Dai, B.B. (2011), "Is the quasi-steady state a real behaviour? A micromechanical perspective", *Géotechnique*, **61**(2), 175-184.
- Yang, J. and Wei, L.M. (2012), "Collapse of loose sand with the addition of fines: the role of particle shape", *Géotechnique*, **62**(12), 1111-1125.
- Yang, J., Wei, L.M. and Dai, B.B. (2015), "State variables for silty sands: Global void ratio or skeleton void ratio?", *Soil. Found.*, **55**(1), 99-111.
- Yang, S.L., Sandven, R. and Grande, L. (2006), "Steady-state lines of sand-silt mixtures", *Can. Geotech. J.*, **43**(11), 1213-1219.
- Yimsiri, S. and Soga, K. (2010), "DEM analysis of soil fabric effects on behaviour of sand", *Géotechnique*, **60**(6), 483-495.
- Zhou, W., Yang, L., Ma, G., Xu, K., Lai, Z. and Chang, X. (2017), "DEM modeling of shear bands in crushable and irregularly shaped granular materials", *Granul. Matter*, **19**: 25.
- Zlatović, S. and Ishihara, K. (1997), "Normalized behaviors of very loose non-plastic soils: effects of fabric", *Soil. Found.*, **37**(4), 47-56.